Monolayer Assembly and Fixation of FePt Nanoparticles: Microstructure and Magnetic Properties

Hanbin Wang,[†,‡] Minjie Zhou,[†] Fujun Yang,[‡] Juan Wang,[†] Yong Jiang,[§] Yi Wang,[‡] Hao Wang,*[,‡] and Quan Li*[,†]

Department of Physics, The Chinese University of Hong Kong, Hong Kong, China, Faculty of Physics and Electronic Technology, Hubei University, Wuhan 430062, China, and School of Materials Science and Engineering, University of Science and Technology Beijing, Beijing 100083, China

Received October 13, 2008. Revised Manuscript Received November 19, 2008

Monolayer-FePt nanoparticles/boron carbide-matrix composite thin films on Si substrate were fabricated by a two-step method. Scanning electron microscopy indicates that the 6 nm FePt nanoparticles are well-separated in the monolayer with an average interparticle distance of <3 nm. Transmission electron microscopy demonstrates that under high temperature annealing, the FePt nanoparticle monolayer possesses good thermal stability against particle sintering. A coercivity of 2200 Oe is obtained for the $Fe_{47}Pt_{53}$ nanoparticle film. The results indicate that the boron carbide could serve as an effective stopper to the FePt grain growth and aggregation and thus contribute to the particle size uniformity and the perseverance of the particle monolayer morphology of the composite film after the high temperature annealing.

Introduction

Storing one data bit in a single tiny grain of magnetic material could facilitate the ultimate in the magnetic storage density, and monolayer assembly of magnetic nanoparticles with uniform size and well-defined particle−particle separation may serve as one of most feasible solutions to achieve such a lofty goal. Among numerous choices of the magnetic materials for such nanoparticles, FePt has aroused much research interest. After Sun's initial demonstration,[1] several groups have realized the controlled chemical synthesis of FePt nanoparticles with monodispersed size, well-defined shape, as well as ordered monolayer assemblies.[2−5] Nevertheless, the low-temperature (<300 °C) synthesis always results in the face-centered cubic (fcc) phase of the FePt, which does not retain its magnetic orientation. High-temperature annealing (usually >500 °C) would cause the Fe and Pt to rearrange themselves within individual particles and form a chemically ordered face-centered tetragonal (fct) structure. The fct-FePt has a large uniaxial anisotropy ($K_u > 5 \times 10^7$ erg/cm^3) that determines its critical diameter as small as ∼3.3 nm,[6] below which thermal fluctuation induces random switching of the magnetization direction. Such small critical diameter makes them extremely attractive in contributing to the storage aerial density improvement. Unfortunately, the high temperature annealing, which is crucial in transforming the magnetically soft fcc- to the useful fct-FePt, would also cause grain growth and aggregation of the nanoparticles, and thus degrades their size uniformity and even destroys the monolayer ordering of the nanoparticles,[7] which two factors are extremely important in permitting smaller data bits to be detected more easily and accurately with existing signal detection and error-correction.

Much effort has been devoted to seeking the solution of such a problem, aiming at self-assembly of the FePt particles with uniform size, well-defined separation, and most importantly, the desired fct phase. Several different approaches have been attempted. Reducing the fcc-fct phase transition temperature via doping/alloying with a third element (such as Ag,[8] Au,[9] Sb,[10] etc.), controlling the Fe/Pt atomic ratio,[11] and the annealing environment[12,13] have been investigated. Some success has been achieved in restricting the grain-growth and aggregation of FePt particles using these methods, but without further demonstrating the monolayer

---

* Corresponding authors. E-mail: liquan@phy.cuhk.edu.hk, wangh@hubu.edu.ch.

[†] The Chinese University of Hong Kong.

[‡] Hubei University.

[§] University of Science and Technology Beijing.

(1) Sun, S.; Murray, C. B.; Weller, D.; Folks, L.; Moser, A. *Science* **2000**, *287*, 1989.

(2) Rong, C. B.; Li, D.; Nandwana, V.; Poudyal, N.; Ding, Y.; Wang, Z. L.; Zeng, H.; Liu, J. P. *Adv. Mater.* **2006**, *18*, 2984.

(3) Chen, M.; Kim, J.; Liu, J. P.; Fan, H. Y.; Sun, S. H. *J. Am. Chem. Soc.* **2006**, *128*, 7132.

(4) Nguyen, H. L.; Howard, L. E. M.; Stinton, G. W.; Giblin, S. R.; Tanner, B. K.; Terry, I.; Hughes, A. K.; Ross, I. M.; Serres, A.; Evans, J. S. O. *Chem. Mater.* **2006**, *18*, 6414.

(5) Yamamoto, S.; Morimoto, Y.; Tamada, Y.; Takahashi, Y. K.; Hono, K.; Ono, T.; Takano, M. *Chem. Mater.* **2006**, *18*, 5385.

(6) Weller, D.; Moser, A.; Folks, L.; Best, M. E.; Lee, W.; Toney, M. F.; Schwickert, M.; Thiele, J. U.; Doerner, M. F. *IEEE Trans. Magn.* **2000**, *36*, 10.

(7) Dai, Z. R.; Sun, S. H.; Wang, Z. L. *Nano Lett.* **2001**, *1*, 443.

(8) Kang, S.; Harrell, J. W.; Nikles, D. E. *Nano Lett.* **2002**, *2*, 1033.

(9) Kang, S. S.; Jia, Z. Y.; Nikle, D. E.; Harrell, J. W. *IEEE Trans. Magn.* **2003**, *39*, 2753.

(10) Yan, Q.; Kim, T.; Purkayastha, A.; Ganesan, P. G.; Shima, M.; Ramanath, G. *Adv. Mater.* **2005**, *17*, 2233.

(11) Varanda, L. C.; Jafelicci, M. *J. Am. Chem. Soc.* **2006**, *128*, 11062.

(12) Li, D.; Poudyal, N.; Nandwana, V.; Jin, Z. Q.; Elkins, K.; Liu, J. P. *J. Appl. Phys.* **2006**, *99*, 08E911.

(13) Sort, J.; Suriñach, S.; Dolors Baró, M.; Muraviev, D.; Dzhardimalieva, G. I.; Golubeva, N. D.; Pomogailo, S. I.; Pomogailo, A. D.; Macedo, W. A. A.; Weller, D.; Skumryev, V.; Nogués, J. *Adv. Mater.* **2006**, *18*, 466.

10.1021/cm802778t CCC: $40.75

assembly of the annealed particles. An alternative approach is to modify the FePt nanoparticle surface and form a core−shell structure,[14−19] with the inert shell protecting the inner FePt core during the annealing process. Although the extent of particle coalescence has been reduced during the heat treatment, the change of FePt surface and widened particle size distribution due to the nonuniformity of the inorganic coating layer make it difficult to further assemble them with the monolayer morphology. In this regard, a polymer mediated approach was presented to obtain self-assembled FePt nanoparticle films with controlled thickness.[20] However, high-temperature annealing resulted in partial or total particle aggregation of the films. Yu et al. took one step forward by decorating the surface of both the FePt nanoparticles and their residing substrate using organic molecules,[21] which process results in the stabilization of the 3.1 nm FePt particles on the Si/SiO_2 substrate upon a vacuum annealing temperature of 800 °C with little aggregation. Nevertheless, the stability of the organic surface coating remains as a problem and the nanoparticle film also suffers from a low coercivity of 110 Oe. Most recently, a miceller approach with SiO_2 thin film capping was proposed to obtain well-dispersed fct-FePt nanoparticle films,[22] with particles demonstrating good thermal stability against grain-growth and aggregation. Although a record coercivity of 1500 Oe has been achieved in such a film, controlling of the Fe/Pt ratio in the particles remain challenging in the one-step fabrication process, and thus make it difficult to optimize the magnetic properties of the film. On the other hand, the overall film's smoothness, chemical stability, and durability are also important factors to be addressed for the desired application. To date, an effective synthesis protocol that could result in the monolayer FePt nanoparticle film with adjustable magnetic properties and other desirable properties is yet to find.

In the present study, we demonstrate the monolayer assembly of uniform FePt nanocube films, which shows little grain-growth and aggregation and possess a coercivity of 2200 Oe after annealing at 650 °C, by a two-step fabrication process. The chemically synthesized FePt nanocubes with a narrow size distribution are first assembled into a monolayer film on the substrate by spin-coating, followed by sputtering deposition of a thin layer of boron carbide (B_4C) as their fixation and protection layer. The choice of B_4C not only effectively protects the FePt nanocubes against coalesce and thus maintain the nanoparticle size uniformity and the monolayer film morphology during the high temperature annealing, but also results in a smooth, chemically stable, and durable composite magnetic film due to the high hardness, good thermal stability (up to 1000 °C), and high oxidation, corrosion, and wear resistance of B_4C.[23]

Experimental Section

FePt Nanoparticle Synthesis. The FePt nanocubes were synthesized by modifying the method reported by Sun.[3] In a typical procedure, a solution of $Pt(acac)_2$, 4 mmol of olcic acid, 4 mmol of oleyl amine, and 2 mmol of $Fe(CO)_5$ in benylether were heated to 200 °C for 2 h under the nitrogen protection. The heating rate was kept at 5 °C per minute below 200 °C. After the prepared black solution was cooled to room temperature, 20 mL of ethanol was added into the solution. The black products were then precipitated by gently centrifugation. The yellow-brownish supernatant was discarded. The precipitate were then redispersed in 10 mL of hexane and precipitated again in 10 mL o fethanol by centrifugation (3000 rpm for 5 min). Further purification of the product was performed by dispersing the product into hexane, precipitating with ethanol, and centrifuging. Finally, the purified nanoparticles were dispersed in 10 mL of hexane.

FePt Nanoparticle Self-Assembly, B_4C Thin Film Deposition, And High-Temperature Annealing. The silicon (001) wafers were first etched by HF solution to remove the surface oxide layer right before the spin-coating process under N_2 protection. A concentration of ~2 mg/mL FePt colloids (FePt nanoparticles dispersed in the mixtures of 1:1 hexane and octane) were used for the spin-coating. A drop of FePt colloid was deposited on the HF-treated Si wafer (~1 × 1 cm) with the spincoater being accelerated to 1500 rpm in 5 s. Circumvolution was maintained at this speed for 80 s. The resulting nanoparticle films were dried under the protection of N_2 at room temperature. A 10 nm B_4C film was deposited using magnetron sputtering with experimental settings described elsewhere.[23] Briefly, a 2.5 in. B_4C (99.5% purity) target was used as the source material, and the FePt nanoparticle-on-Si was used as the substrate. The base pressure of the chamber was 2×10^{-4} Pa and a total pressure of 0.5 Pa was maintained during sputtering. No intentional substrate hearing was employed. Thermal annealing of the particle films was performed after the B_4C film deposition in the same vacuum chamber with a pressure of 1×10^{-5} Pa. The annealing temperature was kept at 650 °C, with one hour duration.

Material Characterization. X-ray diffraction (XRD) was used to determine the crystalline structure of the as-synthesized FePt nanocube powder, and a field-emission scanning electron microscope (SEM, operating at 20 kV) was employed to investigate the morphology of the spin-coated FePt nanocube film on Si. Detailed morphology and microstructure of various samples are characterized using transmission electron microscopy (TEM, Tecnai 20 ST, FEG). Both plan-view and cross-sectional TEM samples are examined, which were prepared by mechanical grinding and polishing followed by low-angle Ar-ion etching. The compositions of the FePt particles were determined using the energy dispersive X-ray (EDX) spectrometer attached to the same microscope. The magnetic properties of the dried fcc FePt nanocube powder and the annealed FePt nanoparticle/B_4C composite film were measured by a physical properties measurement system (PPMS).

---

(14) Yu, C. H.; Caiulo, N.; Chester, C. H.; Lo. Tam, K.; Tsang, S. C. *Adv. Mater.* **2006**, *18*, 2312.

(15) Yan, Q.; Purkayastha, A.; Kim, T.; Kröger, R.; Bose, A.; Ramanath, G. *Adv. Mater.* **2006**, *18*, 2569.

(16) Kang, S. S.; Miao, G. X.; Shi, S.; Jia, Z.; Nikles, D. E.; Harrell, J. W. *J. Am. Chem. Soc.* **2006**, *128*, 1042.

(17) Liu, C.; Wu, X. W.; Klemmer, T.; Shukla, N.; Weller, D. *Chem. Mater.* **2005**, *17*, 620.

(18) Zeng, H.; Li, J.; Wang, Z. L.; Liu, J. P.; Sun, S. H. *Nano lett.* **2004**, *4*, 187.

(19) Caiulo, N.; Yu, C. H.; Yu, K. M. K.; Lo, C. C. H.; Oduro, W.; Thiebaut, B.; Bishop, P.; Tsang, S. C. *Adv. Funct. Mater.* **2007**, *17*, 1392.

(20) Sun, S. H.; Anders, S.; Hamann, H. F.; Thiele, J. U.; Baglin, J. E. E.; Thomson, T.; Fullerton, E. E.; Murray, C. B.; Terris, B. D. *J. Am. Chem. Soc.* **2002**, *124*, 2884.

(21) Yu, A. C. C.; Mizuno, M.; Sasaki, Y.; Inoue, M.; Kondo, H.; Ohta, I.; Djayaprawira, D.; Takahashi, M. *Appl. Phys. Lett.* **2003**, *82*, 4352.

(22) Ethirajan, A.; Wiedwald, U.; Boyen, H. G.; Han, B. K. L.; Klimmer, A.; Weigl, F.; Kästle, G.; Ziemann, P.; Fauth, K.; Cai, J.; Behm, R. J.; Romanyuk, A.; Oelhafen, P.; Walther, P.; Biskupek, J.; Kaiser, U. *Adv. Mater.* **2007**, *19*, 406.

(23) Zhou, M. J.; Li, Q.; Yang, F. J.; Wang, H. B.; Wang, H.; Tang, D. *Appl. Phys. Lett.* **2007**, *91*, 061920.

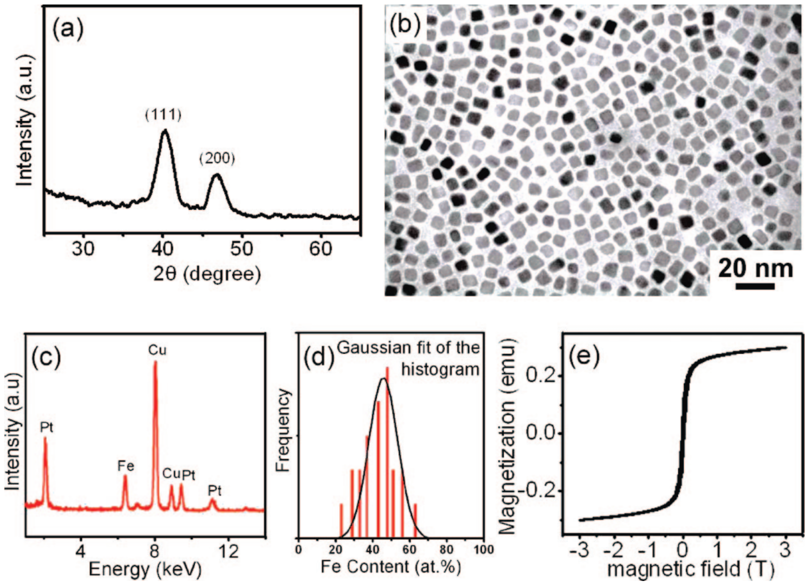

Figure 1. (a) XRD spectrum of the as-synthesized FePt nanoparticles; (b) representative TEM image of the cubical FePt nanoparticles on the carbon-coated copper grid; (c) EDX spectrum of the FePt particles in (b); (d) composition distribution obtained from several tens of individual FePt nanocubes by TEM-EDX analysis. Black curve is the Gaussian fit of the histogram; (e) room-temperature hysteresis loop of the as-synthesized FePt nanoparticle powder.

Results and Discussions

The general crystallinity of the chemically synthesized FePt nanoparticles is disclosed by the powder X-ray diffraction (XRD), as shown in Figure 1a. A broad peak ranging from 38 to 42° and a small peak ranging from 45 to 48° are observed, agreeing with the fcc FePt ⟨111⟩ and ⟨200⟩ reflections, respectively. The average diameter of the particles is estimated as ~6.0 nm on the basis of the Scherrer equation. Both cubelike and spherical FePt nanoparticles can be synthesized by modifying the methods reported by Sun et al.[3] In the present work, we will present our work using the cube-like samples, which morphology can be found in the transmission electron microscopy (TEM) image (Figure 1b) taken from samples dispersed on the carbon film. The size of the nanocubes is ~6 nm with a standard deviation of 11%, agreeing well with the XRD result. The average composition of the nanocubes is estimated as $Fe_{47}Pt_{53}$ from the energy-dispersive X-ray (EDX) results (Figure 1c) with electron probe covering hundreds of such particles. More precise compositional analysis of the nanocubes is obtained by examining the composition of individual particles. Statistic is obtained based on several tens of such nanocubes analyzed (Figure 1d). The majority of the nanocubes has Fe/Pt ratio close to 1, but distribution of the particle composition still exists. Magnetic measurements of these as-synthesized FePt nanocubes (Figure 1e) by physical properties measurement system (PPMS) show that they are soft-magnetic at room temperature, being consistent with what one expects from their fcc structures.

Monolayer assembly of the as-synthesized FePt nanocubes is realized by a precisely controlled spin-coating method, which is found to be effective in producing the monolayer films of FePt nanoparticles on many different substrates including both silicon and silicon dioxide. Here we show our results using the Si substrate. Monolayer formation over 1 × 1 cm^2 area has been achieved, and its typical morphology can be clearly observed in the scanning electron microscopy (SEM) image shown in Figure 2a, in which well-defined particle separation can be observed. Although the monolayer nanoparticle assembly can be achieved over fairly large area (~1 × 1 cm^2), improvement on the uniformity of the surface coverage as well as the assembly ordering is needed.

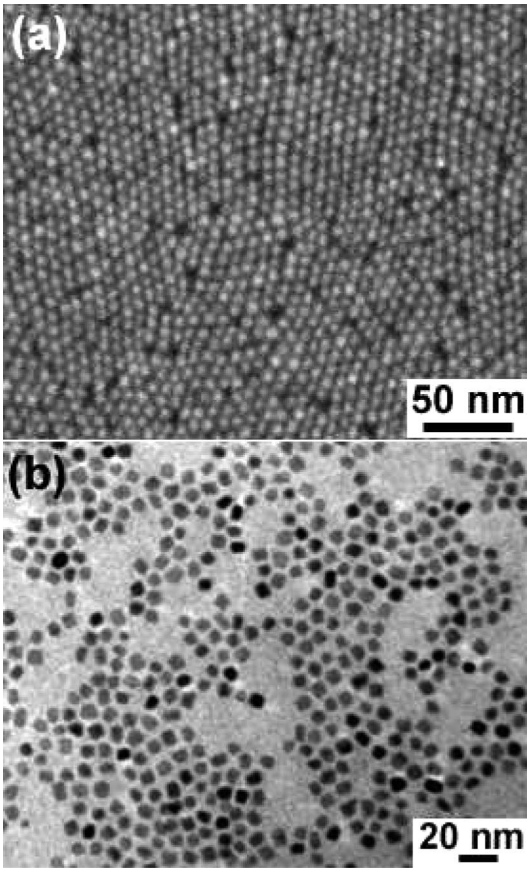

Figure 2. (a) Plan-view high-resolution SEM image of the FePt nanoparticle film without B4C coating; (b) low-magnification plan-view TEM image of the FePt nanoparticle film covered by a 10 nm B4C layer before annealing.

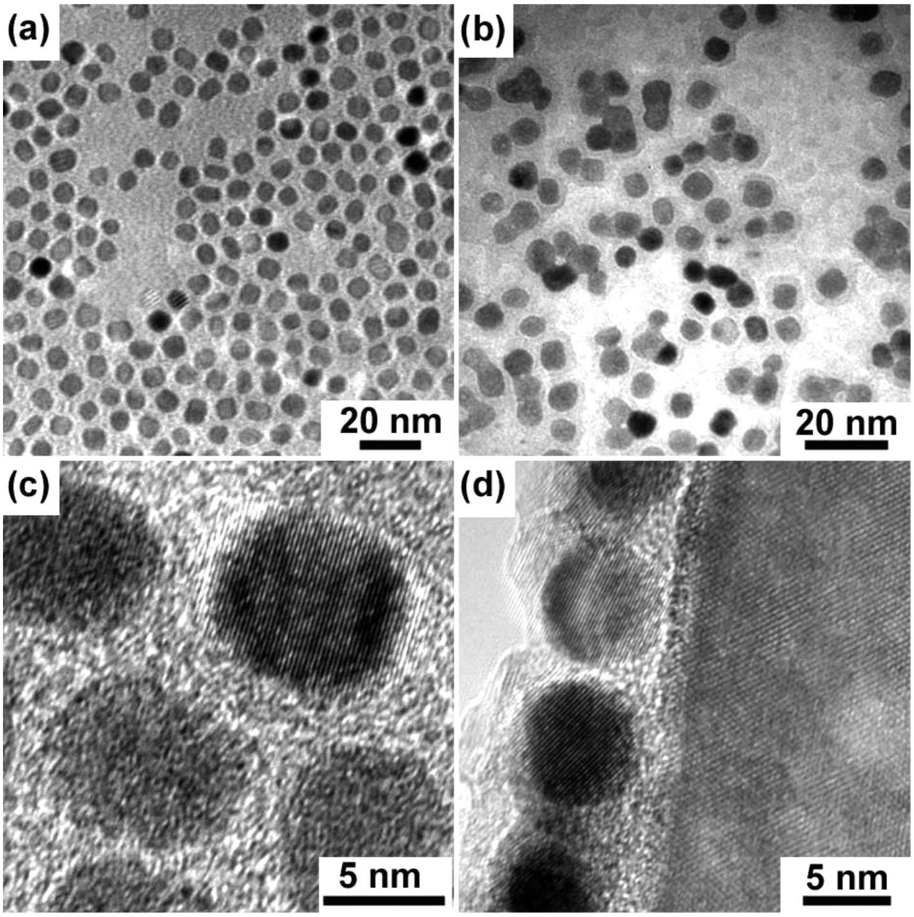

Figure 3. Low-magnification TEM images of Fe47Pt53 nanoparticle film annealed at 650 °C for 60 min (a) under the protection of 10 nm B4C layer and (b) without B4C layer; (c) the plan-view and (d) cross-sectional high-resolution electron microscopy image of the Fe47Pt53-nanoparticle/B4C composite film after annealing.

Effective approaches that could address these problems include surface modifications[24] of the substrate material and Langmuir−Blodgett (LB) techniques,[25] and are currently under investigation. Deposition of a thin layer (10 nm) of B_4C on top of such a monolayer nanoparticle film does not affect the arrangement of the individual FePt nanocubes, which is suggested by the plan-view TEM image (Figure 2b) taken from the B_4C-on-FePt nanocube thin film sample. The FePt nanocubes maintain both their cubical shape and the ∼6 nm size, and remain well-separated with an average interparticle distance of ∼3 nm. Little structure damage is found on the individual nanocubes.

We choose 650 °C as the annealing temperature, which is known to induce the fcc-fct phase transition of the FePt particles.[7,15] On the other hand, aggregation is expected at the same temperature in a conventional FePt nanoparticle system[26] without the protection of a spacer material between individual particles. With amorphous B_4C serving as the fixation and protection layer, little grain growth and aggregation is observed in the nanocube film, with individual FePt particles remain well-separated in the amorphous B_4C matrix with an average separation distance ∼3 nm (Figure 3a), being similar to that before annealing. As a comparison, obvious grain growth and aggregation occur in the monolayer FePt nanoparticle film without the B_4C introduction (Figure 3b). Nevertheless, the morphology of individual FePt nanocubes is indeed affected by the annealing process—the original cubical shape of the as-synthesized FePt particles becomes spherical with the cube corners rounded up (Figure 3c). This is reasonable when considering the rearrangement of the Fe and Pt atoms during the annealing process, which ultimately leads to the fcc−fct phase transition. The high temperature annealing intends to bring the FePt/B_4C thin film system to its thermal equilibrium, when a lowest total energy configuration is preferred. Needless to say, the energy associated with the interface between the FePt nanoparticle and the B_4C matrix contribute to a significant portion of the film's total energy, and a configuration that most likely to minimize the interfacial area and thus the interfacial energy would survive, i.e., spherical shape of the FePt particle. The interface between the FePt nanoparticles and the Si substrate has also been carefully examined. It is interesting to note that a thin amorphous layer forms between the FePt nanoparticles and the Si substrate (Figure 3d). Chemical analysis of such a layer suggests that it contains B and C. Although B_4C was deposited on top of the FePt nanoparticle film, it is possible for B and C

---

(24) Shukla, N.; Svedberg, E. B.; Ell, J. *Surf. Coat. Technol.* **2006**, *201*, 3810.
(25) Pal, P.; Nandi, D.; Misra, T. N. *Thin Solid Films* **1994**, *239*, 138.
(26) Hyun, C.; Lee, D. C.; Israel, C.; Korgel, B. A.; Lozanne, A. D. *IEEE Trans. Magn.* **2006**, *42*, 3799.

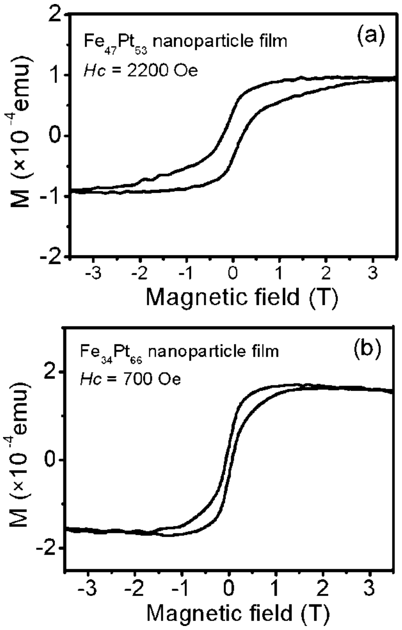

Figure 4. Room-temperature hysteresis loops of the FePt-nanoparticle/B4C composite film with the average Fe/Pt ratio as (a) 47/53 and (b) 34/66, respectively. The films have been annealed at 650 °C for 60 min.

species to diffuse to the original FePt/Si interface, when considering the loose physical absorption of the FePt nanoparticles on the Si substrate, the small diameters of B and C, and the mild substrate heating (~100 °C) during the magnetron sputtering process due to energetic incident ions/atoms from the vapor phase. The formation of such an amorphous layer is actually critical in maintaining the microstructure of the FePt nanoparticle film on Si, as the chemically stable boron carbide layer serves an effective stopper for any possible reactions between Fe/Pt and Si, which is known to occur otherwise.[27,28]

Although one would assume the occurrence of phase transformation from fcc to fct for the monolayer film of FePt nanoparticles at temperatures greater than 500 °C,[8,11] evaluation of the effectiveness of the phase transformation can be obtained only from the magnetic property of the film, i.e., a distinct magnetic hysteresis loop with large coercivity value would definitely suggest the presence of significant amount of fct FePt, and vice versa. The room temperature out-of-plane magnetic hysteresis loops of monlayer-FePt-nanoparticle/B_4C films after annealing are shown in Figure 4. A coercivity of $H_c = 2200$ Oe is obtained for film with average Fe/Pt ratio as 47/53 (Figure 4a). Although such a value is already larger than both the 3.1 nm FePt nanoparticles film obtained via interfacial anchoring layer (110 Oe)[21] and that synthesized by the miceller approach (1500 Oe),[22] it is low when comparing to calculated value of 6 nm fct-FePt nanoparticles. Taking the theoretically determined intrinsic coercivity and magnetocrystalline anisotropy values,[29] a coercivity of 13500 Oe is calculated for fully ordered 6 nm cubical $Fe_{50}Pt_{50}$ particles by using sharrock equation.[30] A number of reasons have been proposed in the literatures to explain the always lower H_c value (compared to the theoretical values), such as the surface oxidation,[31] or the formation of a silicide structure,[27] and the lack of fine control over the Fe/Pt ratio in individual FePt nanoparticles.[32] The first two possibilities are not consistent with our result of the film microstructure, and thus can be excluded. On the other hand, deviation from 1 for the Fe/Pt ratio always exists in individual FePt nanoparticles. As indicated by EDX, even when the average composition of the nanoparticles can be controlled to close to 1 (e.g., in the sample of $Fe_{47}Pt_{53}$), there is always a small portion of Fe_xPt_{100-x} nanoparticles, in which the x value falls beyond the range of $40 < x < 60$. In our experiment, the lack of control on the supply of Fe source ($Fe(CO)_5$) from the vapor phase is considered to be a main factor leading to the inhomogeneous composition distribution of nanoparticles.[33] Consequently, nanoparticle with Fe/Pt ratio significantly deviating from 1 would fail to transform into the hard magnetic phase upon annealing.[34] In fact, we have fabricated similar samples with the average Fe/Pt ratio further deviating from 1 by reducing the dose of $Fe(CO)_5$, and an even lower coercivity of 700 Oe is resulted (Figure 4b). One shall note the unconventional shape of the hysteresis curves shown in Figure 4, particularly in Figure 4b, i.e., the width of the hysteresis loop at finite magnetic moments is greater than that at zero moment. The loops indicate two magnetic phases: the first one is relatively soft and it could be the origin of the slow rotation part of the loops toward the field; the second is the hard one leading to the relatively high coercivity. Similar phenomena have been reported in the literature when measuring the magnetic properties of ~4nm FePt nanoparticle multilayers[35] and 9.5 nm FePt nanoparticles monolayer.[22] As the special line shape of the hysteresis curve suggests the coexistence of magnetic soft (or superparamagnetic) and hard phases, our results then indicate the incomplete fcc-fct phase transformation of the FePt nanoparticles, which is a direct consequence of the Fe/Pt ratio deviation from unity. Further refinement on the chemical synthesis conditions of the FePt nanoparticles to achieve narrower composition distribution is under investigation.

Conclusions

In conclusion, we have demonstrated fabrication of monolayer-FePt nanoparticles/boron carbide composite thin films on Si substrate, which possess good thermal stability and a record coercivity of 2200 Oe for the

---

(27) Thomson, T.; Terries, B. D.; Toney, M. F.; Raoux, S.; Baglin, J. E. E.; Lee, S. L.; Sun, S. *J. Appl. Phys.* **2004**, *95*, 6738.

(28) Yao, B.; Petrova, P. V.; Vanfleet, R. R.; Coffey, K. R. *J. Appl. Phys.* **2006**, *99*, 08E913.

(29) Chantrell, R. W.; Weller, D.; Klemmer, T. J.; Sun, S.; Fullerton, E. E. *J. Appl. Phys.* **2002**, *91*, 6866.

(30) Sharrock, M. P. *IEEE Trans. Magn.* **1990**, *26*, 193.

(31) Anders, S.; Toney, M. F.; Thomson, T.; Farrow, R. F. C.; Thiele, J.-U.; Terris, B. D.; Sun, S.; Murray, C. B. *J. Appl. Phys.* **2003**, *93*, 6299.

(32) Yu, Andrew, C. C.; Mizuno, M.; Sasaki, Y.; Kondo, H. *Appl. Phys. Lett.* **2004**, *85*, 6242.

(33) Saita, S.; Maenosono, S. *Chem. Mater.* **2005**, *17*, 3705.

(34) Stahl, B.; Ellrich, J.; Theissmann, R.; Ghafari, M.; Bhattacharya, S.; Hahn, H.; Gajbhiye, N. S.; Kramer, D.; Viswanath, R. N.; Weissmuller, J.; Gleiter, H. *Phys. ReV. B.* **2003**, *67*, 14422.

(35) Held, G. A.; Zeng, H.; Sun, S. H. *J. Appl. Phys.* **2004**, *95*, 1481.

monolayer FePt nanoparticle thin films. The boron carbide is found to serve as effective stopper to the FePt grain growth and aggregation, and thus contribute to the FePt particle size uniformity and the perseverance of the monolayer particle film morphology after the high temperature annealing (650 °C). The size uniformity of the FePt nanoparticles, the well-defined particle−particle separation, together with the good magnetic property and thermal stability of the overall composite film, make it a very promising candidate for the ultrahigh density magnetic storage media. The combination of conventional solution-based chemical synthesis (for the nanoparticles) and physical vapor deposition (for the fixation/protection layer) in a sequential manner enjoys the advantages of both methods. It can be readily extended to other nanoparticle systems, not only having fine controls over the magnetic particle size, shape, and possibly their individual composition; but also allows a variety of materials to serve as the fixation/protection layer, the correct choice of which guarantee the stability of the monolayer film morphology and its good magnetic property after annealing.

Acknowledgment. This work is supported in part by the Research Grants Council of Hong Kong SAR (ref. 402007), the National Nature Science Foundation of China (50772032 and 50371056), MOST of China (2007CB936202), the Research Fund for the Doctoral Program of China Education Ministry (20060512004), and Natural Science Foundation Creative Team Project of Hubei Province (2007ABC005).

CM802778T